

1-1-2006

Ultraviolet Lasing in High-Order Bands of Three-Dimensional ZnO Photonic Crystals

Michael Scharrer

Alexey Yamilov

Missouri University of Science and Technology, yamilov@mst.edu

Xiaohua Wu

Hui Cao

et. al. For a complete list of authors, see http://scholarsmine.mst.edu/phys_facwork/321

Follow this and additional works at: http://scholarsmine.mst.edu/phys_facwork



Part of the [Physics Commons](#)

Recommended Citation

M. Scharrer et al., "Ultraviolet Lasing in High-Order Bands of Three-Dimensional ZnO Photonic Crystals," *Applied Physics Letters*, American Institute of Physics (AIP), Jan 2006.

The definitive version is available at <https://doi.org/10.1063/1.2203939>

This Article - Journal is brought to you for free and open access by Scholars' Mine. It has been accepted for inclusion in Physics Faculty Research & Creative Works by an authorized administrator of Scholars' Mine. This work is protected by U. S. Copyright Law. Unauthorized use including reproduction for redistribution requires the permission of the copyright holder. For more information, please contact scholarsmine@mst.edu.

Ultraviolet lasing in high-order bands of three-dimensional ZnO photonic crystals

Michael Scharrer, Alexey Yamilov,^{a)} Xiaohua Wu, Hui Cao, and Robert P. H. Chang^{b)}
Materials Research Institute, Northwestern University, Evanston, Illinois 60208

(Received 9 January 2006; accepted 29 March 2006; published online 15 May 2006)

UV lasing in three-dimensional ZnO photonic crystals is demonstrated at room temperature. The photonic crystals are inverse opals with high refractive index contrast that simultaneously confine light and provide optical gain. Highly directional lasing with tunable wavelength is obtained by optical pumping. Comparison of the experimental results to the calculated band structure shows that lasing occurs in high-order bands with abnormally low group velocity. This demonstrates that the high-order band structure of three-dimensional photonic crystals can be used to effectively confine light and enhance emission. Our findings may also impact other applications of photonic crystal devices. © 2006 American Institute of Physics. [DOI: 10.1063/1.2203939]

The development of ultraviolet (UV) microlasers is important for integrated optoelectronics, solid-state lighting, sensors, and other applications. Photonic crystals (PhCs) have great potential to control the functionality and improve performance of such devices. Amplification of light in a PhC can be enhanced by localized defect states inside the photonic band gap¹ (PBG) or via modes with reduced group velocity at a photonic band edge.^{2–4} Both approaches have been applied for quasi-two-dimensional (2D) PhC lasers operating in the near-infrared spectrum.^{5–7} Recent progress has been made in 2D UV-emitting PhC devices based on GaN (Refs. 8 and 9) and ZnO,¹⁰ yet their fabrication presents a considerable challenge due to the required small-scale periodicity. Here we report room-temperature UV lasing in three-dimensional (3D) ZnO PhCs. Unlike previously reported 3D PhC lasers,^{11,12} these structures consist entirely of optically active material. Confinement of light in high-order photonic bands with small group velocity⁴ leads to directional and tunable lasing and a relaxation of the stringent fabrication requirements.

We have recently reported the fabrication of ZnO inverse opals.¹³ ZnO has a wide, direct electronic band gap (~ 3.3 eV) and a high exciton binding energy (~ 60 meV), making it an efficient emission material at near-UV wavelengths. Because ZnO acts as both the dielectric backbone and the gain medium for lasing, we can study the emission properties without having to infiltrate quantum dots^{14,15} or dye molecules.^{11,12} This simplifies the fabrication process and avoids a decrease in refractive index contrast or the degradation of emitters due to interaction with the dielectric backbone.

Our fabrication process is straightforward and applicable to a variety of materials.^{16,17} Polystyrene opal templates are deposited by self-assembly onto glass substrates, infiltrated with ZnO by atomic layer deposition (ALD), and removed by firing at elevated temperatures. The resulting PhC structures are face-centered cubic (fcc) arrays of air spheres surrounded by ZnO dielectric shells with a thickness of typically ~ 50 layers.¹³ Interstitial porosity between the shells is

an inherent feature of the ALD infiltration of an opal lattice, and it leads to beneficial changes in the high-order band structure^{18,19} as discussed below. The refractive index of ZnO is ~ 2.0 in the visible spectrum, but increases to more than 2.5 as λ approaches the excitonic emission wavelength. Although this is not sufficient for the formation of a complete PBG,²⁰ the refractive index contrast is large enough for strong directional gaps.

We can tune the position of the first-order gap throughout the visible spectrum by selecting appropriate polystyrene sphere diameters (i.e., PhC lattice constants) for the opal template.¹³ To study the high-order band structure we used spheres with diameters ranging from $d=330$ nm to 383 nm. The optical effects of high-order bands are more complicated, as shorter waves experience simultaneous Bragg diffraction from multiple sets of lattice planes and coupling of many Bloch modes occurs. Even without a complete PBG, stimulated emission is strongly enhanced in weakly dispersive (“flat”) higher bands,⁴ because the group velocity is reduced over an extended region of k space (group velocity anomaly). Experimentally, high-frequency reflection and transmission spectra of 3D PhCs have been studied,^{21–23} but many of the observed features are not yet fully understood and limited information is available on the effect of the high-order band structure on emission properties.²⁴

Figure 1 shows reflection spectra for light incident along the [111] direction. The first-order Bragg peaks are observed at wavelengths from 655 to 765 nm (peak R1). We also observe two strong reflection peaks (R2 and R3) and several fine features at wavelengths approaching the ZnO absorption edge.

In the lasing experiments, the sample surfaces are illuminated by a white-light source and imaged by a 20 \times objective lens onto a charge coupled device (CCD) camera. Highly reflective areas free of cracks are selected for measurements. The samples are pumped at 10 Hz with 20 ps pulses of $\lambda=355$ nm from a mode-locked Nd:YAG (yttrium aluminum garnet) laser, with a spot diameter of ~ 20 μ m and light incident along the [111] direction. At low pump level the emission spectra of all the samples feature a broad spontaneous emission peak with a maximum at $\lambda \approx 390$ nm. With increasing pump intensity a single lasing peak appears (marked L in Fig. 1), with λ at the short-wavelength edge of

^{a)}Present address: Department of Physics, University of Missouri–Rolla, Rolla, MO 65409.

^{b)}Electronic mail: r-chang@northwestern.edu

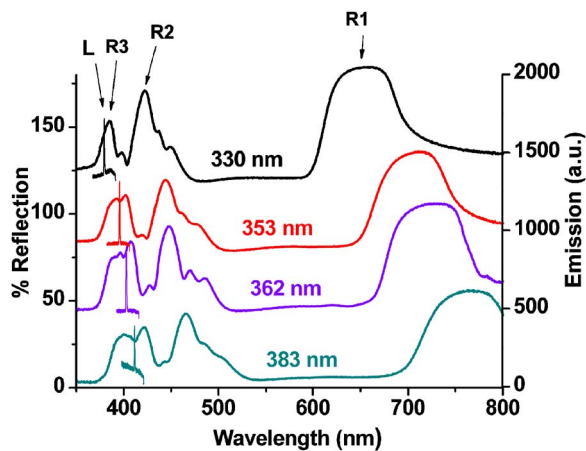


FIG. 1. (Color online) Reflection and lasing spectra of ZnO PhCs for four different sphere diameters. Light is incident along the [111] direction normal to the PhC surface. The first-order Bragg peak (peak R1) and two main reflection peaks at shorter wavelengths (R2 and R3) are detected. Lasing (peak L) occurs at the high-frequency shoulder of the third peak (R3) in all samples.

the third reflection peak. The lasing peak initially has a width of 0.6–1.0 nm, but becomes narrower with increasing pump intensity, reaching a full width at half maximum of 0.1–0.3 nm [Fig. 2(a)]. The emission increases rapidly and shows a pronounced threshold behavior [Fig. 2(a) inset].

Lasing output is highly directional, with a divergence angle of approximately 6° [Fig. 2(b)]. The directionality is preserved if the pump light is incident at an angle slightly off the surface normal. This indicates that lasing is strongly confined in the [111] direction. Changing the PhC lattice constant leads to a shift in lasing wavelength λ_{las} , from $\lambda_{\text{las}} \approx 383$ nm for $d=330$ nm to $\lambda_{\text{las}} \approx 415$ nm for $d=383$ nm

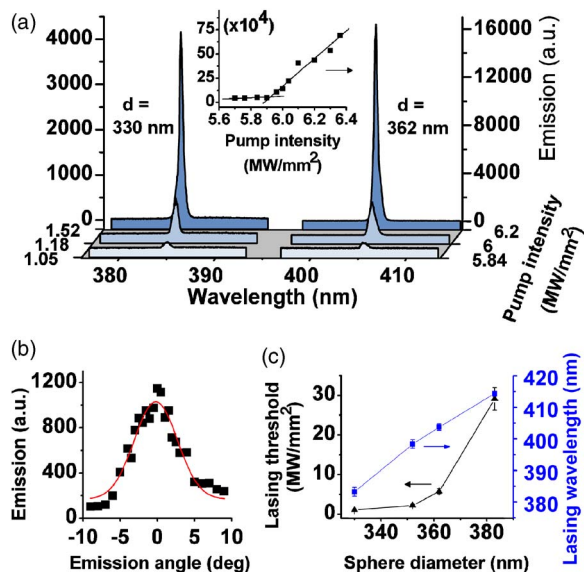


FIG. 2. (Color online) (a) Emission spectra of ZnO PhCs with $d=330$ nm and 362 nm for increasing pump intensity. The peak positions blueshift slightly with increasing pump power. Inset: L - L curve for the 362 nm sample (with a clear threshold at ~ 5.9 MW/mm 2). (b) Angular distribution of lasing emission. 0° corresponds to the [111] direction normal to the sample surface. The emission is strongly directional with a full width at half maximum $\sim 6^\circ$. (Squares represent measured data, the line is a guide for the eye.) (c) Lasing threshold and wavelength vs sphere diameter d . Lasing occurs at longer wavelengths for increasing lattice constants. As the lasing wavelength shifts away from the ZnO gain maximum, the lasing threshold increases sharply.

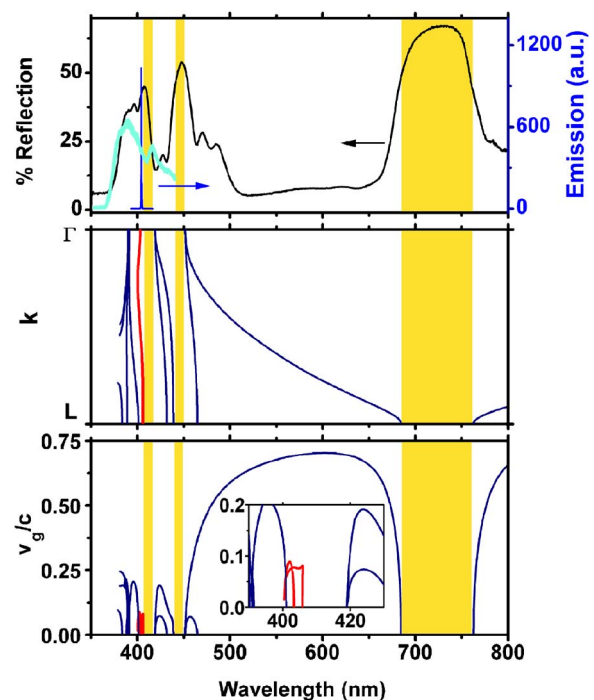


FIG. 3. (Color online) (a) Reflection (black), photoluminescence (light blue), and lasing (dark blue) spectra of a PhC with $d=362$ nm. Lasing occurs at the high-frequency shoulder of the reflection peak at 407 nm. The photoluminescence exhibits a minimum in this region, confirming the existence of a stop band. (b) Calculated band structure of ZnO inverse opals with $d=355$ nm in the Γ - L direction. The lasing peak coincides with the isolated flat band (red) at the high-frequency edge of the third gap. The shaded yellow areas indicate the calculated band gaps. (c) Calculated group velocities. Light in the weakly dispersive band (red) has a very low v_g over the whole Γ - L range.

[Fig. 2(c)], closely matching the shift in the high-order band structure. The gain spectrum of ZnO is centered at ~ 390 nm. Accordingly, the threshold increases with growing distance of λ_{las} from the gain maximum, e.g., by a factor of 30 from $\lambda_{\text{las}} \approx 383$ nm ($d=330$ nm) to $\lambda_{\text{las}} \approx 415$ nm ($d=383$ nm). The fact that lasing occurs at frequencies so far from the gain maximum reveals that the confinement effect of the high-order band structure is remarkably strong in these PhCs. Well above threshold, secondary lasing peaks may appear within a wavelength range of approximately ± 3 nm from the main peak. The exact origin of these peaks is unclear at this time, but our measurements indicate that they are more isotropic and might be caused by defects or lasing in other crystal directions. However, the directional nature of the primary lasing mode, the reproducibility and stability of λ_{las} , and its dependence on the PhC lattice constant suggest that the primary lasing is related to the photonic band structure.

To understand our experimental results, we correlate them to the photonic band structure. Figure 3(a) shows the reflection spectrum of the 362 nm PhC along with lasing and spontaneous emission spectra. The reflection peak at 407 nm coincides with a clear dip in the spontaneous emission spectrum, confirming the existence of a stop band. We have calculated²⁵ the band structure of the inverse opals with interstitial porosity taking into consideration the frequency dependence of the refractive index of ZnO.^{26,27} The calculations were performed for wavelengths longer than 380 nm. We have not accounted for absorption of light, which becomes a dominant effect for shorter wavelengths. The only

adjustable parameter used in the calculations was the sphere diameter d . Figure 3(b) depicts the calculated band structure for wave vectors along the Γ - L $\langle 111 \rangle$ direction for $d = 355$ nm. Three directional band gaps match up closely with the most prominent reflection maxima in the experimental data [Fig. 3(a)]. This correspondence was used as the criterion for determining the fitting parameter d (which is within the margin of uncertainty of sphere diameter, lattice constant after firing, and small variations in filling fraction and topology). The theoretical results can also explain some of the weaker features in the reflection data in terms of band singularities in either Γ or L k directions.

At the high-frequency edge of the third PBG there is an isolated degenerate band (band number 9) with extraordinarily low dispersion which coincides with the lasing wavelength for all our samples. Figure 3(c) plots the calculated group velocity. The ninth band has little overlap with other bands and has a group velocity v_g less than $0.09c$. Light amplification in this band is strongly enhanced due to the extremely low v_g over the whole Γ - L range. This suggests that lasing occurs due to distributed feedback of slow propagating modes in this band. It is worth noting that this flat band is a feature of the inverse opal structure with interstitial porosity and that the corresponding band in a fully filled inverse opal structure shows considerably more curvature. The increase of the refractive index in the vicinity of the electronic band edge leads to additional flattening of the band. Our calculations show that 25%–32% of the energy of a mode in this band is concentrated in the dielectric structure and thus can be efficiently amplified by the gain material.

In summary, we have demonstrated UV lasing in 3D ZnO PhCs at room temperature. Even without a full PBG high-order bands can efficiently confine light in the material and lead to robust and directional lasing. The flat band that we believe is responsible for lasing in our structures lies at the high-frequency edge of the third gap in the $[111]$ direction (between the eighth and the ninth band), where the complete PBG will develop for materials with higher refractive index. Therefore a further decrease in lasing threshold should be possible in systems with higher refractive index contrast or optimized topology.¹⁹ Our results also imply that the high-order photonic band structure of inverse opals can be exploited for photonic applications such as highly efficient LEDs or nonlinear optical processes.

This research project is supported by NSF Grant Nos. ECS-024457 and DMR-0353831, and the use of facilities at the NSF MRSEC program (DMR-0076097) at Northwestern University. The authors thank Larry Aagesen and Katyayani Seal for helpful discussions.

- ¹S. John, Phys. Rev. Lett. **58**, 2486 (1987).
- ²S. Nojima, Jpn. J. Appl. Phys., Part 2 **37**, L565 (1998).
- ³L. Florescu, K. Busch, and S. John, J. Opt. Soc. Am. B **19**, 2215 (2002).
- ⁴K. Sakoda, K. Ohtaka, and T. Ueta, Opt. Express **4**, 481 (1999).
- ⁵O. Painter, R. K. Lee, A. Scherer, A. Yariv, J. D. O'Brien, P. D. Dapkus, and I. Kim, Science **284**, 1819 (1999).
- ⁶H.-G. Park, S.-H. Kim, S.-H. Kwon, Y.-G. Ju, J.-K. Yang, J.-H. Baek, S.-B. Kim, and Y.-H. Lee, Science **305**, 1444 (2004).
- ⁷S. Noda, M. Yokoyama, M. Imada, A. Chutinan, and M. Mochizuki, Science **293**, 1123 (2001).
- ⁸T. N. Oder, J. Shakya, J. Y. Lin, and H. X. Jiang, Appl. Phys. Lett. **83**, 1231 (2003).
- ⁹A. David, C. Meier, R. Sharma, F. S. Diana, S. P. DenBaars, E. Hu, S. Nakamura, C. Weisbuch, and H. Benisty, Appl. Phys. Lett. **87**, 101107 (2005).
- ¹⁰X. Wu, A. Yamilov, X. Liu, S. Li, V. P. Dravid, R. P. H. Chang, and H. Cao, Appl. Phys. Lett. **85**, 3657 (2004).
- ¹¹M. N. Shkunov, Z. V. Vardeny, M. C. DeLong, R. C. Polson, A. A. Zakhidov, and R. H. Baughman, Adv. Funct. Mater. **12**, 21 (2002).
- ¹²W. Y. Cao, A. Munoz, P. Palffy-Muhoray, and B. Taheri, Nat. Mater. **1**, 111 (2002).
- ¹³M. Scharrer, X. Wu, A. Yamilov, H. Cao, and R. P. H. Chang, Appl. Phys. Lett. **86**, 151113 (2005).
- ¹⁴Y. A. Vlasov, K. Luterova, I. Pelant, B. Honerlage, and V. N. Astratov, Appl. Phys. Lett. **71**, 1616 (1997).
- ¹⁵S. G. Romanov, D. N. Chigrin, C. M. S. Torres, N. Gaponik, A. Eychmuller, and A. L. Rogach, Phys. Rev. E **69**, 046606 (2004).
- ¹⁶J. S. King, E. Graugnard, and C. J. Summers, Adv. Mater. (Weinheim, Ger.) **17**, 1010 (2005).
- ¹⁷A. Rügge, J. S. Becker, R. G. Gordon, and S. H. Tolbert, Nano Lett. **3**, 1293 (2003).
- ¹⁸K. Busch and S. John, Phys. Rev. E **58**, 3896 (1998).
- ¹⁹D. Gaillot, T. Yamashita, and C. J. Summers, Phys. Rev. B **72**, 205109 (2005).
- ²⁰H. S. Sozuer, J. W. Haus, and R. Inguva, Phys. Rev. B **45**, 13962 (1992).
- ²¹J. F. Galisteo-Lopez and C. Lopez, Phys. Rev. B **70**, 035108 (2004).
- ²²W. L. Vos and H. M. van Driel, Phys. Lett. A **272**, 101 (2000).
- ²³B. H. Juarez, M. Ibisate, J. M. Palacios, and C. Lopez, Adv. Mater. (Weinheim, Ger.) **15**, 319 (2003).
- ²⁴L. Bechger, P. Lodahl, and W. L. Vos, J. Phys. Chem. B **109**, 9980 (2005).
- ²⁵S. G. Johnson and J. D. Joannopoulos, Opt. Express **8**, 173 (2001).
- ²⁶K. Postava, H. Sueki, M. Aoyama, T. Yamaguchi, C. Ino, Y. Igasaki, and M. Horie, J. Appl. Phys. **87**, 7820 (2000).
- ²⁷The photonic band structure was computed for a set of refractive indices n from 1.8 to 2.5 with 0.05 steps, and linear interpolation was used to obtain $\omega = \omega_{k,i}(n)$, where k is the k vector and i is the band number. Knowledge of ZnO refractive index $n(\omega)$ allows one to obtain $\omega = \omega_{\text{ZnO}}(n)$. By finding the intersection of these functions we determined $\omega_{\text{true}} = \omega_{k,i}(n_{\text{true}})$.